AJNR

Contrast-Enhancement of the Anterior Eye Segment in Patients with Retinoblastoma: Correlation between Clinical, MR Imaging, and Histopathologic Findings

P. de Graaf, P. van der Valk, A.C. Moll, S.M. Imhof, A.Y.N. Schouten-van Meeteren, D.L. Knol and J.A. Castelijns

AJNR Am J Neuroradiol 2010, 31 (2) 237-245
doi: https://doi.org/10.3174/ajnr.A1825
http://www.ajnr.org/content/31/2/237

ORIGINAL RESEARCH

Contrast-Enhancement of the Anterior Eye Segment in Patients with Retinoblastoma: Correlation between Clinical, MR Imaging, and Histopathologic Findings

P. de Graaf
P. van der Valk
A.C. Moll
S.M. Imhof
A.Y.N. Schouten-van Meeteren
D.L. Knol
J.A. Castelijns

FELLOWS' JOURNAL CLUB

BACKGROUND AND PURPOSE: AES contrast-enhancement is recognized in a substantial number of retinoblastoma-affected eyes. We retrospectively investigated the histopathologic basis of AES contrast-enhancement on MR images in retinoblastoma.

MATERIALS AND METHODS: Pretreatment contrast-enhanced MR images were obtained from 42 children with retinoblastoma. Forty-two enucleated eyes were included in this study, AES enhancement was evaluated by using a 3-point score, and these data were correlated with clinical, MR imaging, and histopathologic findings. Additionally, 14 specimens were immunohistochemically analyzed for CD31, VEGF, and Flt-1 expression. Statistical correlations with AES enhancement were assessed by using a linear-by-linear association test and univariate and multivariate ordinal regressions.

RESULTS: The degree of abnormal AES enhancement was moderate in 15 (36%) eyes and strong in 14 (33%) eyes, whereas 13 (31%) eyes showed normal AES enhancement. In multivariate analysis, the degree of AES enhancement showed statistically significant correlations with iris surface-vessel count ($P = .05$) and optic nerve invasion ($P = .04$) in the enucleated eye and with tumor volume ($P = .02$) as detected on MR imaging. No significant associations between AES enhancement and VEGF expression in the iris were observed. Flt-1 ($P = .04$) staining in iris stroma and IA as detected with CD31 staining ($P = .009$) both yielded a statistically significant positive correlation with abnormal AES enhancement.

CONCLUSIONS: The degree of abnormal AES enhancement on MR imaging in retinoblastoma reflects angiogenesis in the iris. AES enhancement is also a hallmark of advanced retinoblastoma because its degree correlates with tumor volume and optic nerve invasion.

ABBREVIATIONS: AC = anterior chamber; AES = anterior eye segment; BOB = blood-ocular barrier; C = cornea; MVD = microvessel density; Flt-1 = VEGF-receptor-1; H&E = hematoxylin-eosin; HIF-1 = hypoxia-inducible factor; HPF = high-power field; IA = iris angiogenesis; IOP = intraocular pressure; VEGF = vascular endothelial growth factor

Conservative treatment strategies can be successful in the avoidance of enucleation and external beam radiation therapy in the early stages of retinoblastoma and in some patients with advanced intraocular disease.[1] As a consequence, more children are treated without histopathologic confirmation of diagnosis and, more important, without knowledge of risk factors for predicting disease dissemination and prognosis. Current histopathologic risk factors for metastasis include invasion to the postlaminar optic nerve, AES, or massive invasion of ocular coats (choroid and sclera).[2-4] MR imaging provides the opportunity for a noninvasive evaluation of these risk factors with reasonable diagnostic accuracy.[5-8]

Tumor angiogenesis is also a histopathologic risk factor for local tumor invasion and systemic dissemination in retinoblastoma[9,10]; initial reports on vascular targeting therapy in mouse models of retinoblastoma show promising results.[11] However, evaluation of angiogenic activity has been performed only in vitro on the histopathology of enucleated eyes. The degree of angiogenesis can be assessed by evaluation of angiogenic markers, such as MVD or expression of VEGF and its receptors.[9,10,12-14] High tumor MVD is correlated to invasive growth and metastasis and is associated with poor prognosis.[9,10] VEGF is highly expressed in retinoblastoma, and in addition to promoting angiogenesis, VEGF causes an increased vascular permeability in neovascular capillary beds with subsequent BOB breakdown.[12-14] Furthermore, released VEGF in the posterior eye segment is able to diffuse into the aqueous of the AC, where it induces IA, spatially separated from the tumor location.[12,14-17] When IA occurs, a membrane of new vessels forms across the iris and AC angle, eventually causing a secondary glaucoma. Retinoblastoma-associated IA, for which enucleation is usually performed, is considered a bad prognostic factor for globe salvage and vision.

Abnormal AES enhancement is present in approximately

Received May 9, 2009; accepted after revision July 10.

From the Departments of Radiology (P.d.G., J.A.C.), Pathology (P.v.d.V.), Ophthalmology (A.C.M., S.M.I.), and Epidemiology and Biostatistics (D.L.K.), VU University Medical Center, Amsterdam, the Netherlands; and Department of Pediatric Oncology (A.Y.N.S.-v.M.), Emma Children's Hospital, Academic Medical Center, Amsterdam, the Netherlands.

P.d.G. is financially supported in part by grants from ZonMw (Netherlands Organization for Health Research and Development), Gravenhage, the Netherlands; ODAS Foundation, Delft, the Netherlands; National Foundation for the Blind and Visually Impaired, Utrecht, the Netherlands; Blindenhulp Foundation, Gravenhage, the Netherlands; and Dutch Eye Fund (grant 2004-23), Utrecht, the Netherlands.

Please address correspondence to Pim de Graaf, MD, Department of Radiology, VU University Medical Center, PO Box 7057, 1007 MB Amsterdam, the Netherlands; e-mail: p.degraaf@vumc.nl

Indicates open access to non-subscribers at www.ajnr.org

DOI 10.3174/ajnr.A1825

22%–41% of MR imaging examinations for retinoblastoma and seems to be an indicator of more aggressive behavior.[6,8,18] Surprisingly, this phenomenon is barely reported in the literature, and underlying pathophysiology and its histopathologic correlates are still unclarified. We postulated that AES enhancement may reflect the status of retinoblastoma-induced IA in vivo. The purpose of our study was to retrospectively investigate the histopathologic basis of abnormal AES enhancement on MR imaging in retinoblastoma.

Materials and Methods

Patient Population

Patients with retinoblastoma who underwent MR imaging between January 1998 and January 2004 were considered for this retrospective study. Patients were included in the study if they met the following criteria: 1) having undergone enucleation of the eye with retinoblastoma, without therapeutic interventions in the affected eye before enucleation; and 2) having undergone pretreatment 1.5T contrast-enhanced MR imaging under general anesthesia, which enabled adequate image interpretation. Forty-eight patients met these inclusion criteria. However, 2 pathologic specimens could not be retrieved from the archives and the quality of 4 pathologic specimens hampered proper analysis, so they were excluded from the study. The final study population consisted of 42 patients with a mean age at MR imaging of 22 months (age range, 2–68 months). There were 18 girls (mean age, 22 months; age range, 2–68 months) and 24 boys (mean age, 21 months; age range, 2–64 months). None of the 7 (17%) bilaterally affected patients underwent enucleation of both eyes. Thus, data obtained about 42 eyes could be evaluated. The right eye was enucleated in 19 (45%) and the left eye, in 23 (55%) patients. The mean interval between MR imaging and enucleation was 5 days (range, 1–12 days). Only 1 (2%) patient showed a positive family history for retinoblastoma.

All patients underwent ophthalmoscopy and sonography after we administered a general anesthetic. In all patients, tumor calcification was documented by using sonography. Medical records were examined by 1 reviewer to assess tumor recurrence or metastases, IOP, presence of vitreous or subretinal tumor seeding, and AES abnormalities, including tumor seeding, AC depth, hypopyon or pseudohypopyon, hyperemia, or IA. Our local ethics committee did not require its approval or informed consent for retrospective review of a patient's records and images.

MR Imaging Technique

MR imaging was performed with 1.5T systems (Vision or Sonata; Siemens, Erlangen, Germany) with use of a head coil. MR imaging included transverse and sagittal spin-echo T1-weighted images (TR/TE, 500/15 ms; 4 acquisitions), transverse spin-echo T2-weighted images (TR/TE, 2000–2700/60 ms [intermediate-weighted images] and 2000–2700/120 ms [T2-weighted images], 1 acquisition), followed by fat-suppressed spin-echo T1-weighted images (TR/TE, 575/15 ms; 3 acquisitions) in 3 directions obtained shortly after intravenous administration of 0.2 mmol/L gadolinium chelate (Magnevist; Schering, Berlin, Germany) per kilogram of body weight. For all sequences, section thickness was 3 mm, with a 0.3-mm intersection gap.

Image Analysis

MR images were reviewed by 2 observers with 16 and 7 years of experience with orbital MR imaging. Both observers were blinded to the original MR imaging reports and clinical and histopathologic information. T2-weighted images were used to assess retinal detachment (no detachment, some amount of detachment, or total detachment) and decreased AC depth (yes/no). The latter was assessed by a visual comparison with the contralateral AC. On T1-weighted images obtained before and after contrast material injection, an independent evaluation was conducted of the degree of AES enhancement with a 3-point scale: strong (equal to or greater than the intensity of choroidal enhancement), moderate (less than choroidal enhancement), and normal AES enhancement (no perceptible enhancement within the AES) (Fig 1). After completing image interpretations, the 2 reviewers compared their independent results and discrepancies were resolved in consensus.

Tumor-volume measurements were performed by 1 observer on contrast-enhanced axial T1-weighted images with use of a computerized image-analysis tool that is available as part of the PACS of our hospital (Centricity Radiology RA 600; GE Healthcare, Milwaukee, Wisconsin). In every section in which tumor was present, this struc-

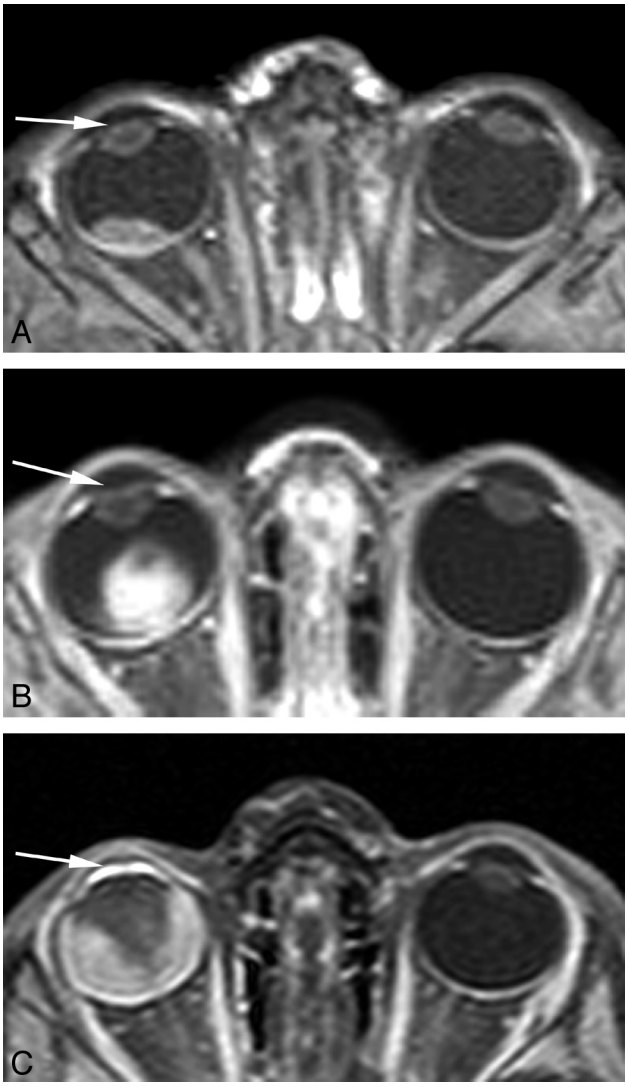

Fig 1. Transverse contrast-enhanced T1-weighted fat-suppressed spin-echo MR images of 3 different patients with unilateral retinoblastoma of the right eye show the grading of AES enhancement on a 3-point scale: normal AES enhancement (no perceptible enhancement within the AES) (*A, arrow*); moderate AES enhancement (less than choroidal enhancement) (*B, arrow*); and strong AES enhancement (equal to or greater than the intensity of choroidal enhancement) (*C, arrow*). All the unaffected (left) eyes show normal AES enhancement.

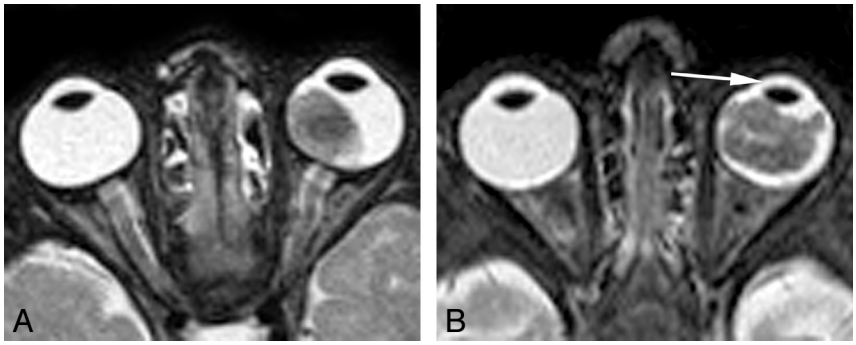

Fig 2. Transverse T2-weighted spin-echo MR images of 2 different patients with unilateral retinoblastoma of the left eye. *A,* A large intraocular retinoblastoma and a normal AC depth in comparison with the unaffected right eye. *B,* A large intraocular retinoblastoma and a decrease in AC depth (*arrow*) in comparison with the unaffected right eye.

ture was manually surrounded by a region of interest. Surfaces of regions of interest were automatically calculated, and all surfaces in different sections were summed afterward and multiplied by section thickness and intersection gap. Tumor volumes were categorized into 4 subgroups[6]: very small, <0.65 cm^3; small, 0.65–1.30 cm^3; medium, >1.30–1.95 cm^3; and large, >1.95 cm^3.

Histopathologic Analysis

One pathologist with 11 years' experience in ophthalmopathology, who was blinded to patients' clinical records and MR imaging findings, specifically re-evaluated all included eyes. Histopathologic evaluation, by using H&E staining, included the following: localization of tumor bulk with respect to the equator (anterior, posterior, or a combination); amount of tumor necrosis (semiquantitatively estimated according to the percentage of necrotic tumor area); involvement of choroid (inflammation, minimal or massive tumor invasion), sclera, ciliary body, AES, and optic nerve invasion (pre- or postlaminar). One or 2 sections of each specimen showing representative parts of the iris were judged microscopically at $\times$40 magnification for the presence of IA. IA classification was based on groups defined by Pe'er et al[12]: 0, no angiogenesis; 1, fine isolated capillaries with the normal iris structure remaining intact; 2, a layer of thin capillaries covering the iris surface; and 3, a prominent vascular membrane with flattening of the iris surface with or without ectropion uvea. In 5 high-power fields (original magnification, $\times$40), the total number of iris vessels and the number of vessels directly beneath the anterior iris surface were counted. Neovessels (Pe'er 1–3) outside the anatomic anterior iris surface were not included in both vessel counts.

Immunohistochemical Staining

Only 16 formalin-fixed and paraffin-embedded archival tissue blocks still contained some iris tissue and could, therefore, be retrieved from the pathology archives for additional immunohistochemical staining. Deparaffinized 4-μm sections were immunohistochemically stained by using the avidin-biotin-peroxidase complex and direct antibodies against CD31 (DAKO, Glostrup, Denmark), VEGF (Santa Cruz Biotechnology, Santa Cruz, California) and Flt-1 (Santa Cruz Biotechnology). Appropriate negative and positive controls were used throughout. Additionally, 2 specimens contained a large amount of iris pigment, which hampered proper analysis, so they were excluded from immunohistochemical analysis. In this small subgroup of 14 eyes, classification of IA was repeated on CD31-stained specimens. Evaluation of VEGF and Flt-1 staining intensity in the iris was graded as follows: negative, weak, or strong.

Statistical Analysis

All statistical calculations were performed by using SPSS, Version 12.0 (SPSS, Chicago, Illinois). Interobserver agreement of the MR imaging analysis regarding AES enhancement and AC depth was calculated by using the weighted Cohen κ with squared loss. κ values <0.40 were considered to indicate poor agreement; 0.41–0.60, moderate; 0.61–0.80, substantial; and >0.81, excellent agreement.[19] For statistical associations with AES enhancement, the linear-by-linear association test was performed for categoric variables; and ordinal regression, for continuous variables. Finally, a stepwise multivariate ordinal regression of AES enhancement on variables found to have a statistically significant association with it in the univariate analyses was calculated. Statistical comparisons for immunohistochemical data were performed by using the Spearman rank correlation. Log- and square-root transformations of variables were performed when appropriate. A P value $< .05$ was considered statistically significant.

Results

Clinical Findings

Mean follow-up time after enucleation was 83 months (range, 47–130 months). During follow-up, 1 patient (2%) developed histologically confirmed local recurrence. In 20 (48%) eyes, IOP was not measured. Mean IOP was 19 mm Hg; and in 8 (36%) eyes, IOP was elevated ($>$22 mm Hg). Tumor seeding to the vitreous and subretinal space was present in 18 (43%) and 14 (33%) eyes, respectively. Clinically, we noted the following findings in the anterior segment: hypopyon, 1 (2%) eye; hyperemia, 7 (17%) eyes; IA, 2 (5%) eyes; and tumor seeding, 1 (2%) eye. AC depth was decreased in 7 (17%) eyes.

MR Imaging Findings

Retinal detachment was observed in 31 (74%) eyes, of which 14 (45%) eyes showed a total detachment. A shallow AC was detected on MR imaging in 12 (29%) eyes (Fig 2). Abnormal contrast enhancement in the AES was observed in 29 (69%) eyes. The enhancement was classified as moderate in 15 (36%) and strong in 14 (33%) eyes (Fig 3*A*). Agreement between the 2 observers in the assessment of AES parameters, AC depth ($\kappa = 0.84$) and contrast-enhancement of the AES ($\kappa = 0.89$), was very good. Mean tumor volume was 1326.6 mm^3. In 6 (14%) eyes, mean tumor volume was very small; in 16 (38%), it was small; in 13 (31%), it was medium; and in 7 (17%), it was large.

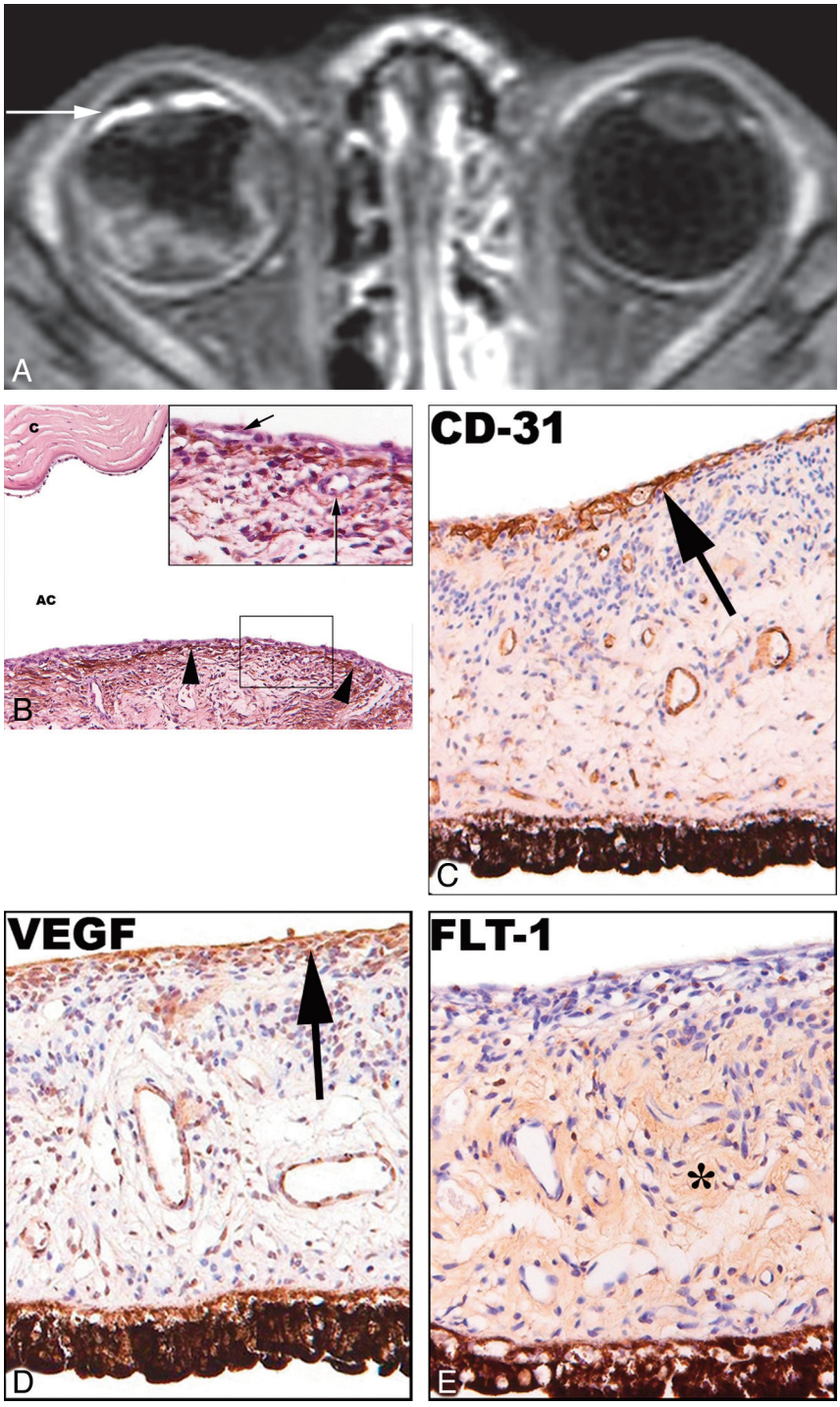

Fig 3. Unilateral retinoblastoma in a 29-month-old boy (case 12). *A,* Transverse contrast-enhanced T1-weighted fat-suppressed spin-echo MR image shows a retinal detachment (*arrow*), with diffuse retinal thickening and enhancement due to retinoblastoma in the affected right eye. Compared with AES of the normal left eye, a strong abnormal enhancement is shown in the right eye. *B,* Histopathologic specimen of the iris, AC, and C, with details of the anterior iris surface (inset). The anatomic anterior surface of the iris (*arrowheads*) is covered by a prominent vascular membrane of newly formed capillaries (*short arrow*) (IA, Pe'er stage 3). Some vessels are present directly beneath the anatomic anterior iris surface (*long arrow*) (H&E, original magnification ×20 objective). *C,* IA at the anterior iris surface (*arrow*) is confirmed on additional CD31 staining (*arrow*) (×40 objective). *D* and *E,* VEGF expression in the iris is particularly present in the anterior part of the iris (*arrow*), and Flt-1 expression shows a widespread staining of the iris stroma (*asterisk*).

Histopathologic Findings

Retinoblastoma was located anterior to the equator in 4 (10%) eyes, and tumor growth from posterior to anterior beyond the equator was observed in 14 (33%) eyes. The mean amount of tumor necrosis was 26.7%. Minimal choroidal inflammation was observed in 9 (21%) eyes; and tumor invasion, in 9 (21%) eyes. Massive choroidal invasion or scleral invasion, both important metastatic risk factors, did not occur in our study population. The extent of optic nerve invasion was prelaminar in 17 (41%) eyes and postlaminar in 3 (7%) eyes. AES invasion was found histopathologically in 1 (2%) eye. IA was classified as stage 0 in 28 (67%) eyes, stage 1 in 9 (21%) eyes, stage 2 in 4

Table 1: Distribution of contrast enhancement in the AES in relation to clinical findings in 42 eyes with retinoblastoma[a]

Variable	Normal (n = 13)	Moderate (n = 15)	Strong (n = 14)	P Value
Tumor recurrence				1.00
Yes	0 (0)	1 (7)	0 (0)	
No	13 (100)	14 (93)	14 (100)	
Intraocular pressure				.61
Unknown	9 (69)	7 (47)	4 (29)	
Mean ± SD (mm Hg)	11.8 ± 5.7	24.1 ± 9.6	19.0	
Range (mm Hg)	7–20	11–36	10–37	
Vitreous seeding				.17
Yes	3 (23)	8 (57)	7 (54)	
No	10 (77)	6 (43)	6 (46)	
Subretinal seeding				.31
Yes	6 (46)	5 (36)	3 (23)	
No	7 (54)	9 (64)	10 (77)	
Anterior chamber seeding				1.00
Yes	0 (0)	1 (7)	0 (0)	
No	13 (100)	14 (93)	14 (100)	
Anterior chamber depth				.07
Shallow	0 (0)	3 (20)	4 (29)	
Normal	13 (100)	12 (80)	10 (71)	
Pseudohypopyon				1.00
Yes	0 (0)	1 (7)	0 (0)	
No	13 (100)	14 (93)	14 (100)	
Hyperemia				.20
Yes	0 (0)	4 (27)	3 (21)	
No	13 (100)	11 (73)	11 (79)	
IA				.20
Yes	0 (0)	0 (0)	2 (14)	
No	13 (100)	15 (100)	12 (86)	

[a] Unless otherwise indicated, data are the number of eyes, and numbers in parentheses are percentages.

Table 2: Distribution of contrast enhancement in the AES in relation to MR imaging findings in 42 eyes with retinoblastoma[a]

Variable	Normal (n = 13)	Moderate (n = 15)	Strong (n = 14)	P Value
Retinal detachment				.17
Total detachment	2 (15)	6 (40)	6 (43)	
Some amount of detachment	7 (54)	4 (27)	6 (43)	
No detachment	4 (31)	5 (33)	2 (14)	
Anterior chamber depth				.02
Shallow	1 (8)	4 (27)	(50)	
Normal	12 (92)	11 (73)	7 (50)	
Tumor volume[b]				.002
Mean ± SD (mm^3)	932.8 ± 561.3	1492.7 ± 617.4	1514.4 ± 388.7	
Range (mm^3)	221.5–1845.0	523.6–2463.5	910.5–2106.8	
Very small	5 (38)	1 (7)	0 (0)	
Small	5 (38)	6 (40)	5 (36)	
Medium	3 (23)	3 (20)	7 (50)	
Large	0 (0)	5 (33)	2 (14)	

[a] Unless otherwise indicated, data are the number of eyes, and numbers in parentheses are percentages. Percentages may not add up to 100% because of rounding.
[b] Log-transformed.

(10%) eyes, and stage 3 in 1 (2%) eye. The mean iris vessel count and mean iris surface vessel count of 42 eyes were determined as 81.1 and 8.7, respectively.

Correlation of AES Enhancement with Clinical, MR Imaging, and Histopathologic Findings

Clinical, MR imaging, and histopathologic findings and results of univariate statistical comparisons between the degree of AES enhancement and clinical, MR imaging, and histopathologic variables are described in Tables 1–3, respectively. The number of eyes with abnormal AES enhancement increased with increasing tumor volume. Very small tumors showed an abnormal (moderate) AES enhancement in only 1 (17%) eye. Small, medium, and large tumors showed moderate AES enhancement in 38%, 23%, and 71%, respectively. Strong AES enhancement occurred in 14 eyes, and tumor volume was >0.65 cm^3 in all of these eyes. Furthermore, all large tumors (volume >1.95 cm^3) showed some degree of abnormal AES enhancement. In the absence of abnormal AES enhancement, there was no tumor invasion of the AES or postlaminar optic nerve, whereas 2 (15%) eyes showed prelaminar optic nerve invasion and 4 (31%) eyes showed minimal choroidal invasion.

A shallow AC as detected on MR imaging (P = .02), and tumor volume (P = .002) as well as histopathologic optic nerve invasion ($P < 0.0001$) and mean iris surface vessel count ($P < 0.0001$) (Fig 3*B*) all yielded a statistically significant positive association with AES enhancement. Choroidal inflammation (P = .02) showed a significant correlation with normal AES enhancement. A shallow anterior chamber as detected during clinical examination (P = .07) and histopathologic IA (Pe'er classification) (P = .06) (Fig 3*B*) showed a trend toward an association with AES enhancement. In multivariate ordinal regression, tumor volume (P = .02), optic nerve invasion (P = .04), mean iris surface-vessel count (P = .05), and choroidal inflammation (P = .002) remained significant.

Correlation of AES enhancement and Immunohistochemical Findings

Immunohistochemical findings are summarized in Table 4. IA as detected with CD31 immunoreactivity was classified as Pe'er stage 0 in 7 (50%) eyes, 1 in 3 (21%) eyes, 2 in 2 (14%) eyes, and 3 in 2 (14%) eyes (Fig 3*C*). Only 1 (20%) eye showed early-stage IA in the absence of abnormal AES enhancement, and 1 (25%) eye showed extensive IA in the group of moderate AES enhancement. Furthermore, a strong AES enhancement was associated with some degree of IA in all 5 eyes. IA as detected with CD31 immunoreactivity yielded a statistically significant positive correlation with AES enhancement (r = 0.665; P = .009) (Figs 4 and 5).

The iris showed VEGF immunoreactivity in all 14 eyes, with 12 (86%) eyes showing anterior iris surface staining (Fig 3*D*) and 8 (57%) eyes showing iris stroma staining. No significant associations between AES enhancement and VEGF expression in the iris were found. Iris stroma showed Flt-1 staining in 12 (86%) eyes, whereas the anterior iris surface was negative in 10 (71%) eyes. The correlation between Flt-1 staining in the iris stroma and AES enhancement was significant (r = 0.555; P = .04) (Fig 3*E*).

Discussion

Three previous studies draw attention to abnormal AES enhancement, which is present in a substantial number of MR images of eyes harboring retinoblastoma.[6,8,18] Authors of these studies correlated AES enhancement with clinical and

Table 3: Distribution of contrast enhancement in the AES in relation to histopathologic findings in 42 eyes with retinoblastoma[a]

Variable	Normal (n = 13)	Moderate (n = 15)	Strong (n = 14)	P Value
Tumor location				.88
Anterior to equator	2 (15)	1 (7)	1 (7)	
Posterior to equator	8 (62)	8 (53)	8 (57)	
Combination	3 (23)	6 (40)	5 (36)	
Necrosis				.56
Mean ± SD	24.6 ± 20.0	34.0 ± 21.2	20.7 ± 11.9	
Range	5–60	5–70	10–50	
Choroidal inflammation				.02
Yes	5 (39)	4 (27)	0 (0)	
No	8 (62)	11 (73)	14 (100)	
Choroidal invasion				.17
Massive	0 (0)	0 (0)	0 (0)	
Minimal	4 (31)	4 (27)	1 (7)	
No	9 (69)	11 (73)	13 (93)	
Scleral invasion				1.00
Yes	0 (0)	0 (0)	0 (0)	
No	13 (100)	15 (100)	14 (100)	
AES				1.00
Yes	0 (0)	1 (7)	0 (0)	
No	13 (100)	14 (93)	14 (100)	
Optic nerve invasion				<.0001
Postlaminar	0 (0)	1 (7)	2 (14)	
Prelaminar	2 (15)	5 (33)	10 (71)	
No	11 (85)	9 (60)	2 (14)	
IA				.06
Stage 3	0 (0)	0 (0)	1 (7)	
Stage 2	0 (0)	3 (20)	1 (7)	
Stage 1	1 (8)	4 (27)	4 (29)	
Stage 0	12 (92)	8 (53)	8 (57)	
Iris vessel count/5 HPF				.18
Mean ± SD	75.8 ± 11.9	83.9 ± 14.6	83.2 ± 14.6	
Range	56–93	47–102	66–124	
Iris surface-vessel count/5 HPF				<.0001[b]
Mean ± SD	3.7 ± 2.8	9.5 ± 6.6	12.8 ± 9.5	
Range	0–9	1–26	1–32	

[a] Unless otherwise indicated, data are the number of eyes, and numbers in parentheses are percentages.
[b] Square-root transformed for statistical analysis because of skewed distribution.

histopathologic findings. De Graaf et al[6] reported the clinical presence of IA, hyperemia, or inflammation as possible explanations for AES enhancement. Galluzzi et al[18] published a series of 16 eyes and found a correlation between histopathologic optic nerve and/or choroid invasion and AES enhancement on MR imaging; however, no correlation between clinical or histopathologic presence of IA and AES enhancement could be detected. On the other hand, Brisse et al[8] could not confirm this correlation between AES enhancement and optic nerve invasion in 10 eyes. To our knowledge, the present investigation is the most comprehensive study so far in the search for an explanation for variable AES enhancement in retinoblastoma, which confirmed the role of IA in vivo. Additionally, our study indicates that abnormal AES enhancement in retinoblastoma is also related to tumor volume and optic nerve invasion.

In healthy human eyes, the uveal tract enhances after intravenous administration of gadolinium contrast material, with the choroid and ciliary body enhancing slightly more than the iris. In the literature,[21,22] there is evidence for an anterior diffusional pathway that causes diffusion of proteins (and gadolinium) from the choroid into the AC. This diffusion goes from the ciliary body vessels, via the ciliary body stroma, into the root of the iris and finally into the AC. A gradual signal-intensity increase in the AC, as a result of diffusion of gadolinium into the AC is physiologic (anterior diffusional pathway). However, this physiologic diffusion is much slower than the enhancement described earlier. First, this enhancement becomes detectable at the AC angle ~12 minutes after injection and moves slightly toward the AC center (~30 minutes), reaching a peak in ~74 minutes.[21,22] However, in our patients, the MR images were obtained shortly after contrast material injection and showed an early signal-intensity increase in the AC of 69% of affected eyes. This early enhancement has been attributed to leakage of contrast material into the extravascular space through regions of BOB disruption.[18,23] In newly formed capillaries during IA, the BOB is poorly developed from the outset and becomes further compromised under hypoxic conditions, with VEGF as an important mediator.

Tumor hypoxia initiates compensatory mechanisms that prevent cell death, including up-regulation of proangiogenic factors, such as VEGF, which are highly expressed in areas of novel vasculature in eyes containing retinoblastoma.[12-14] We found a positive iris VEGF staining in most of the eyes, being more frequent at the anterior iris surface than in the iris stroma. However, no significant correlation between iris VEGF expression and AES enhancement could be detected. This could be explained by the fact that the study population did not include very early stages of retinoblastoma, because these patients are currently treated with eye-preserving strategies. A significant percentage of retinoblastoma eyes succumbing to enucleation demonstrate a high level of VEGF expression.[12-14] Different angiogenic mechanisms might be differentially important in various stages of tumor progression, and some data suggest that VEGF may be especially important in the initial stages.[24] Two human tyrosine kinases, Flt-1 and KDR, have been shown to function as specific receptors for VEGF-related angiogenesis.[25] In the present investigation, only Flt-1 was analyzed because the expression of Flt-1, but not that of KDR, is directly up-regulated by hypoxia.[26] Flt-1 expression is up-regulated by hypoxia via a HIF-1-dependent mechanism, and the expression is also potentiated by VEGF.[26] Hypoxia-induced up-regulation of Flt-1 could provide a mechanism by which local sensitivity to VEGF is enhanced, with increased angiogenesis and vascular permeability as a consequence. In the iris, a positive Flt-1 staining at the level of the iris stroma yielded a significant correlation with AES enhancement, which is a bit surprising because a receptor is expected to bind to cells. We assume that cellular protrusions are the basis for this staining, though staining of a soluble form of Flt-1 in the stroma cannot be excluded.

The degree of AES enhancement correlated significantly with vascular proliferation on the inner as well as on the outer surface of the anatomic anterior iris border.

The mean number of iris vessels located directly beneath the anterior surface was higher in the abnormal AES enhancement groups than in the group with normal AES enhancement. Furthermore, increased AES enhancement showed a similar relationship with the histopathologic stage of IA on the outer surface. This relationship showed a borderline significance for the entire study group but reached statistical signif-

Table 4: Immunohistochemical findings in 14 eyes with retinoblastoma

Case No./Sex/ Age (mo)	AES	VEGF		Flt-1		CD31
	Enhancement	Iris Surface	Iris Stroma	Iris Surface	Iris Stroma[a]	IA[b]
1/M/2	Normal	Strong	Weak	Weak	Weak	1
2/F/25	Normal	Weak	Negative	Negative	Negative	0
3/M/4	Normal	Strong	Weak	Weak	Weak	0
4/M/12	Normal	Negative	Negative	Negative	Negative	0
5/M/31	Normal	Strong	Weak	Negative	Weak	0
6/F/26	Moderate	Weak	Negative	Negative	Weak	0
7/F/16	Moderate	Strong	Weak	Strong	Weak	3
8/F/2	Moderate	Strong	Weak	Negative	Weak	0
9/M/2	Moderate	Strong	Strong	Negative	Weak	0
10/M/36	Strong	Weak	Negative	Negative	Weak	1
11/F/20	Strong	Negative	Negative	Negative	Weak	2
12/M/29	Strong	Weak	Negative	Negative	Weak	3
13/M/6	Strong	Strong	Weak	Strong	Strong	2
14/M/3	Strong	Strong	Weak	Negative	Weak	1

[a] Significant correlation between AES enhancement and the data in this column ($r = .555$; $P = .04$)
[b] Significant correlation between AES enhancement and the data in this column ($r = .665$; $P = .009$). IA according to the Pe'er classification.[12]

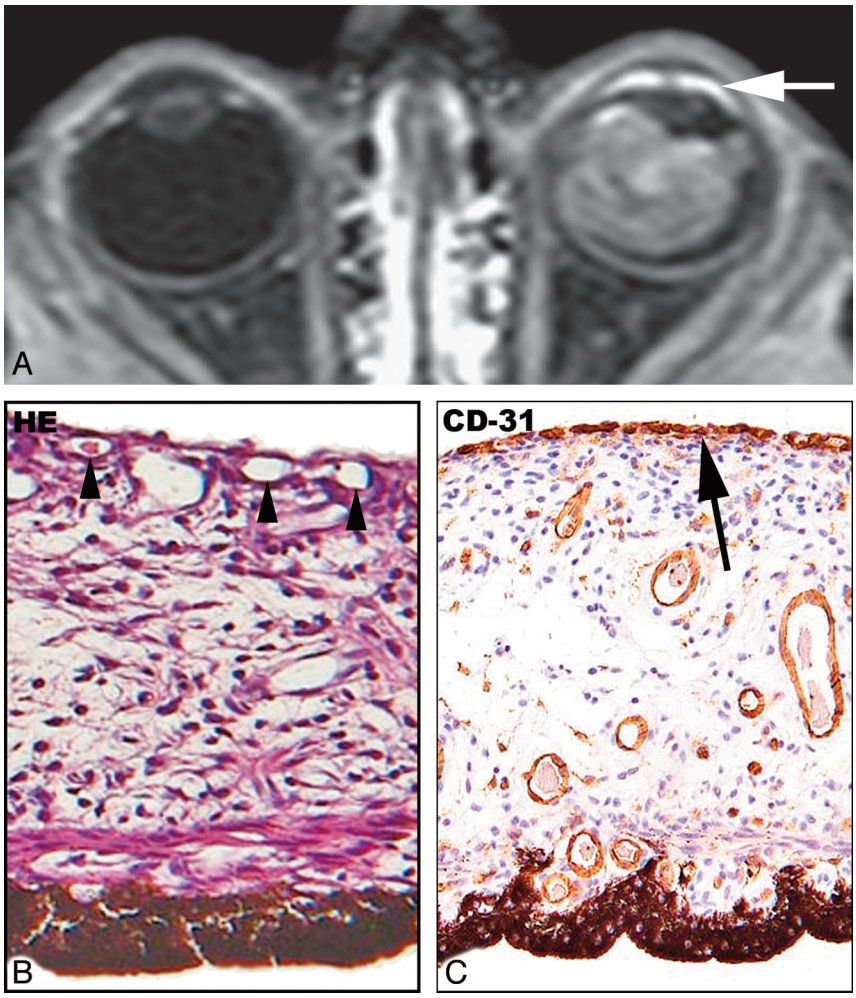

Fig 4. Unilateral retinoblastoma in a 6-month-old boy (case 13). *A*, Transverse contrast-enhanced T1-weighted fat-suppressed spin-echo MR image shows a large enhancing tumor mass in the left eye combined with a strong abnormal enhancement of the AES (*arrow*). *B*, Histopathologic specimen shows detail of the iris. Marked increase of blood vessels directly beneath the anatomic anterior iris surface (*arrowheads*) is present in this part of the iris (H&E, original magnification ×40 objective). *C*, CD31 staining shows a layer of fine capillaries (*arrow*) covering the anatomic anterior iris surface (IA, Pe'er stage 2) (original magnification ×40 objective).

icance with immunohistochemical analysis, probably because CD31 antibody staining is supposed to be more sensitive for the detection of vessels than H&E staining,[27] providing a more accurate discrimination of IA subgroups.

Clinically, retinoblastoma-associated IA, for which enucleation is usually performed, especially in patients with unilateral disease, is considered a bad prognostic factor for globe salvage and vision. However, routine ophthalmoscopy has a

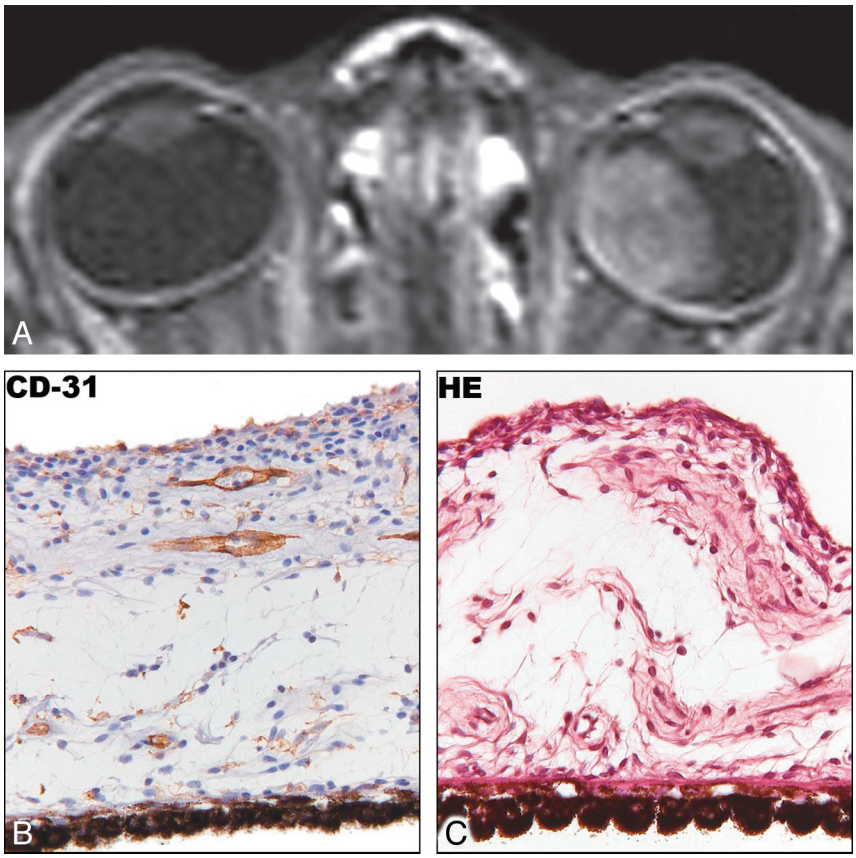

Fig 5. Unilateral retinoblastoma in a 2-month-old boy (case 5). *A*, Transverse contrast-enhanced T1-weighted fat-suppressed spin-echo MR image shows a large enhancing tumor mass in the left eye. Symmetric normal enhancement of the AES of both eyes is shown. *B*, Histopathologic specimen shows details of the iris with a normal aspect of the anterior surface (H&E, original magnification ×40 objective). *C*, CD31 staining shows the absence of vessels outside the anterior iris surface (no IA, Pe'er stage 0) (original magnification ×40 objective).

low sensitivity for detecting early or subtle stages of IA, a finding confirmed in our study (2 eyes with IA detected clinically, compared with 14 eyes detected histopathologically).[18,28] The degree of AES enhancement might be a valuable diagnostic parameter in the choice between enucleation and conservative treatment strategies. Normal AES enhancement seems to be an indication for considering globe salvage rather than enucleation. Abnormal AES enhancement, especially in eyes showing a strong enhancement, represents a sign of IA and could be considered an additional argument in favor of enucleation.

Tumors with increased angiogenesis have a greater potential for tumor progression, invasion of surrounding structures, and metastasis.[9,10] In our study, patients with an advanced stage of disease, indicated by a large tumor volume or the presence of optic nerve invasion, showed a higher degree of AES enhancement, compared with those with early-stage disease. All eyes containing large tumors showed some degree of abnormal AES enhancement, whereas this finding was uncommon in very small and small tumors.

Optic nerve invasion beyond the lamina cribrosa is one of the most important risk factors for extraocular relapse; and as observed before,[18] an abnormal AES enhancement should prompt a radiologist to be suspicious of optic nerve invasion. In the absence of abnormal AES enhancement, there was no tumor invasion of the optic nerve to a postlaminar degree.

Hypoxic conditions in retinoblastoma, secondary to the overgrowth of its vasculature, cause tumor necrosis and enhance angiogenic activity in the posterior segment as well as the AES, with the induction of IA and BOB disruption as a consequence. Pe'er et al[12] found a strong association between higher stages of IA in eyes containing tumors with greater amounts of necrosis. Our study material showed no differences between the amounts of necrosis in the various AES enhancement groups. Theoretically, retinal hypoxia secondary to retinal detachment may also cause BOB disruption and IA. Although retinal detachment was a frequent finding in our study population (74%), with a substantial amount of total detachments, we failed to demonstrate a significant association with AES enhancement.

A shallow AC was clinically demonstrated in 7 patients, whereas evaluation of MR imaging depicted it in 12 patients. In univariate statistical analysis, AES enhancement correlated statistically significantly only with a shallow AC as detected on MR imaging. Possibly, MR imaging is more sensitive in detecting minor anterior displacement of the lens-iris diaphragm, because this parameter can be judged on transverse cross-sectional images.

Inflammation and angiogenesis are linked processes, regulated by inflammatory cytokines and VEGF.[25,29] An increased uveal enhancement, including the AES, was reported as a sign of choroidal inflammation.[6] Surprisingly, we found a significant inverse correlation between AES enhancement and choroidal inflammation. Angiogenesis and inflammation are multistep processes influenced by an imbalance between positive and negative regulators produced by both tumor cells and

normal cells. Regulatory proteins other than VEGF, which show mutually opposing functions of stimulating angiogenesis and inhibiting inflammation, might play an additional role.[30,31] Furthermore, the AES is not always involved in posterior uveitis; therefore, differences in the extent and severity of uveal contrast enhancement depend on the severity of BOB breakdown in the AES.[32]

Limitations to this study are primarily related to the retrospective design. Currently, the use of orbital surface coils is recommended for retinoblastoma imaging to increase spatial resolution and signal–to-noise ratio.[5,7] Future research on retinoblastoma-associated BOB impairment and quantification of leakage across the endothelium should be performed with dynamic contrast-enhanced MR imaging, which is widely used for tumor imaging.[33] Contrast-enhanced MR imaging seems to be a useful tool for noninvasive detection of retinoblastoma-related angiogenesis and could define a subgroup of patients who would potentially profit from vascular targeting drugs in the future.[11,34]

In conclusion, the degree of abnormal AES enhancement on MR imaging in retinoblastoma reflects angiogenesis in the iris. AES enhancement is also a hallmark of advanced retinoblastoma because its degree correlates with tumor volume and optic nerve invasion.

References

1. Lumbroso-Le Rouic L, Aerts I, Levy-Gabriel C, et al. **Conservative treatments of intraocular retinoblastoma**. *Ophthalmology* 2008;115:1405–10
2. Chantada GL, Dunkel IJ, Antoneli CB, et al. **Risk factors for extraocular relapse following enucleation after failure of chemoreduction in retinoblastoma.** *Pediatr Blood Cancer* 2007;49:256–60
3. Chantada GL, Casco F, Fandino AC, et al. **Outcome of patients with retinoblastoma and postlaminar optic nerve invasion.** *Ophthalmology* 2007;114:2083–89
4. Uusitalo MS, Van Quill KR, Scott IU, et al. **Evaluation of chemoprophylaxis in patients with unilateral retinoblastoma with high-risk features on histopathologic examination.** *Arch Ophthalmol* 2001;119:41–48
5. Schueler AO, Hosten N, Bechrakis NE, et al. **High resolution magnetic resonance imaging of retinoblastoma.** *Br J Ophthalmol* 2003;87:330–35
6. de Graaf P, Barkhof F, Moll AC, et al. **Retinoblastoma: MR imaging parameters in detection of tumor extent.** *Radiology* 2005;235:197–207
7. Lemke AJ, Kazi I, Mergner U, et al. **Retinoblastoma: MR appearance using a surface coil in comparison with histopathological results.** *Eur Radiol* 2007; 17:49–60
8. Brisse HJ, Guesmi M, Aerts I, et al. **Relevance of CT and MRI in retinoblastoma for the diagnosis of postlaminar invasion with normal-size optic nerve: a retrospective study of 150 patients with histological comparison.** *Pediatr Radiol* 2007;37:649–56
9. Marback EF, Arias VE, Paranhos A Jr, et al. **Tumour angiogenesis as a prognostic factor for disease dissemination in retinoblastoma.** *Br J Ophthalmol* 2003;87:1224–28
10. Rossler J, Dietrich T, Pavlakovic H, et al. **Higher vessel densities in retinoblastoma with local invasive growth and metastasis.** *Am J Pathol* 2004; 164:391–94
11. Jockovich ME, Suarez F, Alegret A, et al. **Mechanism of retinoblastoma tumor cell death after focal chemotherapy, radiation, and vascular targeting therapy in a mouse model.** *Invest Ophthalmol Vis Sci* 2007;48:5371–76
12. Pe'er J, Neufeld M, Baras M, et al. **Rubeosis iridis in retinoblastoma: histologic findings and the possible role of vascular endothelial growth factor in its induction.** *Ophthalmology* 1997;104:1251–58
13. Kvanta A, Steen B, Seregard S. **Expression of vascular endothelial growth factor (VEGF) in retinoblastoma but not in posterior uveal melanoma.** *Exp Eye Res* 1996;63:511–18
14. Stitt AW, Simpson DA, Boocock C, et al. **Expression of vascular endothelial growth factor (VEGF) and its receptors is regulated in eyes with intra-ocular tumours.** *J Pathol* 1998;186:306–12
15. Kuchle M, Vinores SA, Green WR. **Immunohistochemical evaluation of the integrity of the blood-aqueous barrier in normal and rubeotic human eyes.** *Graefes Arch Clin Exp Ophthalmol* 1995;233:414–20
16. Miller JW, Adamis AP, Shima DT, et al. **Vascular endothelial growth factor/vascular permeability factor is temporally and spatially correlated with ocular angiogenesis in a primate model.** *Am J Pathol* 1994;145:574–84
17. Tolentino MJ, Miller JW, Gragoudas ES, et al. **Vascular endothelial growth factor is sufficient to produce iris neovascularization and neovascular glaucoma in a nonhuman primate.** *Arch Ophthalmol* 1996;114:964–70
18. Galluzzi P, Cerase A, Hadjistilianou T, et al. **Retinoblastoma: abnormal gadolinium enhancement of anterior segment of eyes at MR imaging with clinical and histopathologic correlation.** *Radiology* 2003;228:683–90. Epub 2003 Jul 24
19. Landis JR, Koch GG. **The measurement of observer agreement for categorical data.** *Biometrics* 1977;33:159–74
20. Freddo TF. **Shifting the paradigm of the blood-aqueous barrier.** *Exp Eye Res* 2001;73:581–92
21. Bert RJ, Caruthers SD, Jara H, et al. **Demonstration of an anterior diffusional pathway for solutes in the normal human eye with high spatial resolution contrast-enhanced dynamic MR imaging.** *Invest Ophthalmol Vis Sci* 2006; 47:5153–62
22. Bert R, Freddo T, Caruthers SD, et al. **Confirmation of an anterior large-molecule diffusion pathway in the normal human eye.** *Invest Ophthalmol Vis Sci* 1999;40(suppl):S198
23. Chen CJ. **Intraocular contrast enhancement in Adams pattern III hypoxic brain damage: MRI.** *Neuroradiology* 2000;42:54–55
24. Kerbel R, Folkman J. **Clinical translation of angiogenesis inhibitors.** *Nat Rev Cancer* 2002;2:727–39
25. Penn JS, Madan A, Caldwell RB, et al. **Vascular endothelial growth factor in eye disease.** *Prog Retin Eye Res* 2008;27:331–71
26. Ferrara N. **Vascular endothelial growth factor: basic science and clinical progress.** *Endocr Rev* 2004;25:581–611
27. Vermeulen PB, Gasparini G, Fox SB, et al. **Second international consensus on the methodology and criteria of evaluation of angiogenesis quantification in solid human tumours.** *Eur J Cancer* 2002;38:1564–79
28. Ino-ue M, Azumi A, Shirabe H, et al. **Iridopathy in eyes with proliferative diabetic retinopathy: detection of early stage of rubeosis iridis.** *Ophthalmologica* 1998;212:15–18
29. Imhof BA, Aurrand-Lions M. **Angiogenesis and inflammation face off.** *Nat Med* 2006;12:171–72
30. Matsubayashi R, Matsuo Y, Edakuni G, et al. **Breast masses with peripheral rim enhancement on dynamic contrast-enhanced MR images: correlation of MR findings with histologic features and expression of growth factors.** *Radiology* 2000;217:841–48
31. Teraoka H, Sawada T, Nishihara T, et al. **Enhanced VEGF production and decreased immunogenicity induced by TGF-beta 1 promote liver metastasis of pancreatic cancer.** *Br J Cancer* 2001;85:612–17
32. Brancato R, Bandello F, Lattanzio R. **Iris fluorescein angiography in clinical practice.** *Surv Ophthalmol* 1997;42:41–70
33. Rebeles F, Fink J, Anzai Y, et al. **Blood-brain barrier imaging and therapeutic potentials.** *Top Magn Reson Imaging* 2006;17:107–16
34. Jubb AM, Oates AJ, Holden S, et al. **Predicting benefit from anti-angiogenic agents in malignancy.** *Nat Rev Cancer* 2006;6:626–35